WILEY ONLINE LIBRARY
Early View publication on wileyonlinelibrary.com
(issue and page numbers not yet assigned;
citable using Digital Object Identifier – **DOI**)

Phys. Status Solidi RRL, 1–11 (2012) / **DOI** 10.1002/pssr.201206393

Part of Focus Issue on
Topological Insulators – From Materials Design to Reality
Eds.: Claudia Felser, Shoucheng Zhang, Binghai Yan

pss +++rapid research letters+++
www.pss-rapid.com

Review@RRL

Topological insulator nanostructures

Judy J. Cha[1], Kristie J. Koski[1], and Yi Cui[*, 1, 2]

[1] Materials Science and Engineering, Stanford University, 476 Lomita Mall, Stanford, CA 94305, USA
[2] Stanford Institute for Materials and Energy Sciences, SLAC National Accelerator Laboratory, 2575 Sand Hill Road, Menlo Park, CA 94025, USA

Received 16 September 2012, revised 12 October 2012, accepted 16 October 2012
Published online 24 October 2012

Keywords topological insulators, nanostructures, Bi_2Se_3, transport

[*] Corresponding author: e-mail yicui@stanford.edu, Phone: 650 723 4613, Fax: 650 725 4034

Topological insulators provide a gateway to investigate fundamental quantum behaviours of exotic quasi-particles as well as the promise to revolutionize modern technology. This is due to their unique surface states that are robust against time reversal perturbation and exhibit unique spin-momentum locking property. Enhancing the surface state signal in proportion to the bulk of the material is critical to study the surface states and for future electronics applications. This can be achieved by making topological insulators into nanostructures, which have large surface to volume ratios thus maximizing the topological surface state signal. This article reviews the recent progress made in topological insulator nanostructures including chemical and physical synthesis techniques to make topological insulator nanostructures, notable transport experiments, and current efforts to protect the surface states from degradation. Lastly, future transport studies using topological insulator nanostructures and various chemical methods to tune their materials properties for diverse electronic applications are suggested.

1 Introduction Topological insulators (TIs) are recently discovered quantum materials that are insulating in the bulk, but conductive on the surface [1–3]. Gapless surface states in TIs originate from strong spin–orbit coupling in the bulk, and exhibit special electronic property of spin-momentum locking due to time reversal symmetry. The exotic electronic nature of the TI surface states has garnered intense interests in this new class of materials and can be used to study several fundamental physical phenomena inaccessible in ordinary materials. The spin-momentum locking property of the TI surface states will undoubtedly be useful for a broad range of future electronic applications such as dissipationless transport, spintronics, and quantum computing.

In this review, we follow the recent experimental research progress in TI nanostructures, and discuss various nanomaterial synthesis methods and notable transport measurements. Also, current materials challenges that hinder the easy access and control of the TI surface states are identified and unique solutions that TI nanostructures can provide to overcome these challenges are suggested. The basic concept of TIs is covered very briefly; interested readers can find excellent review articles elsewhere [4, 5]. For comparison with TI nanostructures, several key experimental results on TI bulk crystals and thin films are listed, but not discussed in detail. We finish the review with a materials perspective to look at how the materials properties of the TI nanostructures can be widely tuned using various chemical methods.

2 Topological invariants and edge boundaries

The discovery of a quantum Hall state [6] has led to an effort to classify electronic structures according to what are called topological invariants [7]. Under this classification, an ordinary band insulator is topologically different from a quantum Hall state whose inner part is also insulating. The gapless, conducting edge in the quantum Hall state is a manifestation of the change of the topological invariant at the interface between an ordinary insulator (air) and a two-dimensional (2D) TI [1]. Building upon this idea, it was found that, in the absence of strong magnetic fields, a combination of strong spin–orbit interactions and time re-

versal symmetry can make a 3D TI with a topological invariant that is different from a normal band insulator [8]. Spin-resolved, gapless surface states can therefore emerge in the 3D TI material at the interface between an ordinary insulator (air) and the TI, as illustrated schematically in Fig. 1(a) and (b).

A non-trivial topological insulating phase was first demonstrated in HgTe/CdTe semiconductor quantum wells [3], which are technically challenging to grow. Two years later (2009), three binary chalcogenides, Sb_2Te_3, Bi_2Te_3, and Bi_2Se_3, were predicted as 3D TIs with the TI surface states having a single Dirac cone (Fig. 1(c) and (d)) [9]. This theoretical work boosted interest in TIs as experimentalists rushed to verify the existence of surface states in these traditionally well-known binary compounds.

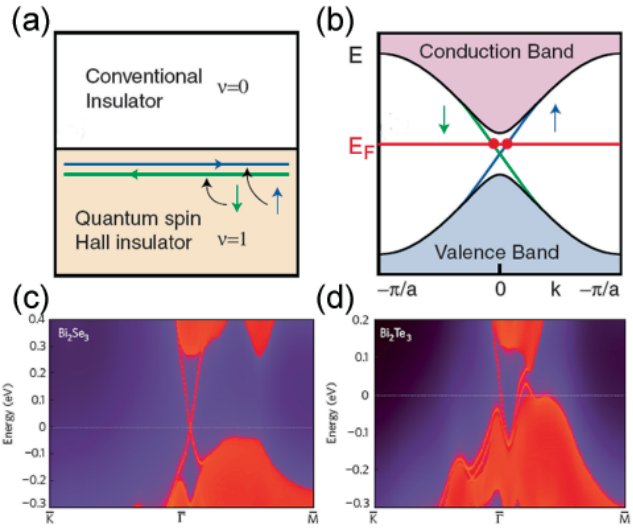

Figure 1 (online color at: www.pss-rapid.com) (a) Edge states form at the interface between a conventional insulator (topological invariant of zero) and a topological insulator (topological invariant of one). They are spin-resolved as denoted by two separate channels (green and blue). (b) Edge states possess momentum-spin locking property where the spin of the electron is determined by the direction of motion. (c) Local density of states of Bi_2Se_3 on the [111] surface shows a surface state with a Dirac electronic dispersion. (d) Local density of states of Bi_2Te_3 on the [111] surface also shows a surface state with the Dirac point embedded in the bulk valence band. (a) and (b) Reprinted Fig. 5 with permission from Ref. [4], copyright (2010) by the American Physical Society. (c) and (d) Reprinted with permission from Macmillan Publishers Ltd., Ref. [9], copyright (2009).

Two essential electronic properties exist for the TI surface states. First, momentum along the surface is well-defined and has a one-to-one correlation with spin. Second, non-magnetic disorder or impurities cannot make the TI surface states localized or gapped due to time reversal symmetry. In other words, the surface state is topologically protected. The spin-momentum locking property and the robustness of the TI surface states make the 3D TI an ideal candidate for various fundamental studies [10] as well as a broad range of technological applications [11].

3 Experimental results in bulk crystals and thin films Following theoretical predictions, experiments on 3D TIs quickly proceeded in bulk TI crystals and thin films grown by molecular beam epitaxy (MBE). In this section, we highlight notable early experiments on TI bulk crystals and thin films, which have confirmed the predicted electronic properties of the TI surface states.

Judy J. Cha is a post-doctoral researcher in the Department of Materials Science and Engineering at Stanford University, CA, USA. She received her Ph.D. in Applied Physics from Cornell University, Ithaca, NY, USA in 2009. Her research focuses on synthesis and transport measurements of two-dimensional nanochalcogenides, in particular topological insulator nanoribbons and nanoplates. She also uses analytical scanning transmission electron microscopy and electron energy-loss spectroscopy to characterize the synthesized nanomaterials.

Kristie J. Koski is a post-doctoral researcher in the Department of Materials Science and Engineering at Stanford University, CA, USA. She received her Ph.D. in Chemistry from University of California, Berkeley, CA in 2008. As a physical chemist, her research focus is in two-dimensional layered nanomaterials including developing new synthetic growth methods, new methods to chemically tune these nanomaterials – especially in the development of new methods of intercalation chemistry, and in the investigation of the unusual physics and chemistry exhibited in these materials.

Yi Cui is an Associate Professor and David Filo and Jerry Yang Faculty Scholar in the Department of Materials Science and Engineering at Stanford University and SLAC National Accelerator Laboratory. His current research is on nanomaterials for energy storage, photovoltaics, topological insulators, biology and environment. He received his Ph.D. in Chemistry from Harvard University and was a Miller Postdoctoral Fellow at University of California, Berkeley. He is an Associate Editor of *Nano Letters*. He is a co-director of the Bay Area Photovoltaics Consortium. He has founded Amprius Inc., a company to commercialize the high-energy battery technology. He has received the Wilson Prize (2011), the Sloan Research Fellowship (2010), KAUST Investigator Award (2008), ONR Young Investigator Award (2008), MDV Innovators Award (2007), Terman Fellowship (2005), and the Technology Review World Top Young Innovator Award (2004).

3.1 Spectroscopic studies Initial experiments to study the TI surface states employed spectroscopic techniques on bulk TI crystals and thin films. TI surface states of Bi_xSb_{1-x}, Bi_2Se_3, and Bi_2Te_3 were directly visualized by angle-resolved photoemission spectroscopy (ARPES) [12–14], confirming the linear band dispersion and spin-momentum locking property of the surface states [15, 16]. Scanning tunneling spectroscopy was used to confirm the linear band dispersion in Bi_2Se_3 independently [17] and to show suppression of backscattering events in Bi_xSb_{1-x} [18]. Soon after, a gap opening in the TI surface states of Bi_2Se_3, induced by coupling between the top and bottom TI surface states [19] and by magnetic dopants [20, 21], was observed using ARPES.

3.2 Transport measurements Following successful spectroscopic studies, several transport measurements on TI bulk crystals, such as Bi_2Se_3, Bi_2Te_3, and Bi_2Se_2Se, reported two-dimensional Shubnikov-de Hass (SdH) oscillations to indicate the presence of conducting surface electrons [22–25]. Gate-dependent SdH oscillations are currently being investigated in nano-sized materials to confirm the Dirac nature of the TI surface states via transport [26]. Nanostructures are used because, in bulk crystals, tuning the Fermi level via field-effect gating is weak because of the large bulk volume.

In thin films, weak anti-localization was observed to show that electron carriers experienced large spin–orbit interactions, an essential ingredient for TIs [27, 28]. A crossover from weak anti-localization to localization was demonstrated in Cr-doped Bi_2Se_3 film and Fe-decorated Bi_2Te_3 film [29, 30], which showed that magnetic impurities, such as Cr and Fe, could induce a gap in the otherwise gapless TI surface states by breaking time reversal symmetry. The anomalous Hall effect has also been observed when magnetic moments are induced in TI materials [31]. An effort to observe the quantum anomalous Hall effect [32] in magnetically doped TIs is ongoing. Topological superconductors either by intercalating Cu in the van der Waals gaps of Bi_2Se_3 [33–35] or by proximity effect [36] are also being actively researched.

A serious challenge in studying the TI surface states via transport is the relatively large residual bulk carriers that dominate the transport signal. Ideally, TIs should be bulk insulators. However, significant residual bulk carriers are unavoidable in real TI materials due to crystal defects such as Se vacancies in Bi_2Se_3 and anti-site defects in Bi_2Te_3. Effective tuning of the Fermi energy via compensation doping in bulk crystals [23, 37], compositional tuning in MBE-grown $(Bi_{1-x}Sb_x)_2Te_3$ thin films [38], and field-effect gating in thin films [39] has been shown to reduce the bulk carriers significantly, but not completely. In Bi_2Te_2Se bulk crystals, the bulk carrier mobility was intentionally made extremely low, compared to the TI surface state mobility, so that the high bulk carrier density became irrelevant [24, 25]. Despite this progress, better TI materials with truly insulating bulk (or, minimal contribution from the bulk carriers) are still lacking. Future transport studies should investigate the topological nature of the surface states in detail such as the robustness of the spin-momentum locking property and suppression of backscattering under various conditions. These may be difficult in current bulk crystals as the contribution of the surface states to transport is limited due to the residual bulk carriers; thus, investigations in nanomaterials may provide this insight.

4 TI nanostructures TI nanostructures offer several advantages over their bulk counterparts for investigating the fundamental nature of the TI surface states and for a broad range of technological applications. The most obvious advantage of a nanomaterial is enhanced surface effects due to the large surface-to-volume ratio. Several groups have made TIs into nanostructures such as exfoliated flakes from bulk crystals [40] and nanoribbons [41] and nanoplates [42]. The large surface-to-volume ratio in nanostructures serves them as a valid platform to study the topological nature of the surface states.

Single-crystalline nanomaterials are routinely obtained by various nanomaterial synthetic techniques [43, 44], with crystalline quality comparable to bulk synthesized materials. Various dopants and growth substrates can be incorporated in nanomaterial synthesis for a diverse set of electrical and optical properties. Heterostructures of multiple nanomaterials, either in a core/shell arrangement [45] or in stacking of different nanomaterials along the length of the nanowire [46], are also routinely carried out. Thus, supreme-quality nanomaterials can be used as ideal platforms to study fundamental condensed matter physics questions. An excellent example is the recent transport measurements on InSb nanowires with superconducting leads to investigate Majorana fermions [47].

Another advantage that nanostructures offer for TI studies over bulk crystals and thin films is their unique morphology. TI nanostructures have well-defined morphology at the nanoscale, such as nanowires, nano-hexagons, nano-triangles, and nanoribbons whose cross-sections follow the symmetry of the underlying crystal structure. This results in transport conditions in which the TI surface electrons are forced to travel in a well-defined path at the nanoscale, ideal for interference-type experiments of the TI surface electrons such as Aharonov–Bohm (AB) oscillations [48, 49].

4.1 Physical synthesis Various synthesis methods are available to make TI nanomaterials. Broadly, we divide the methods into two categories: dry, physical synthesis and wet, chemical synthesis. Physical synthesis includes mechanical exfoliation and nanomaterial synthesis such as vapor–liquid–solid (VLS) [41, 50], vapor–solid (VS) [42, 51, 52], and metal-organic chemical vapor deposition (MOCVD) [53] methods. The mechanical exfoliation method is the so-called scotch tape method [40, 54], adopted from the graphene community [55, 56], where

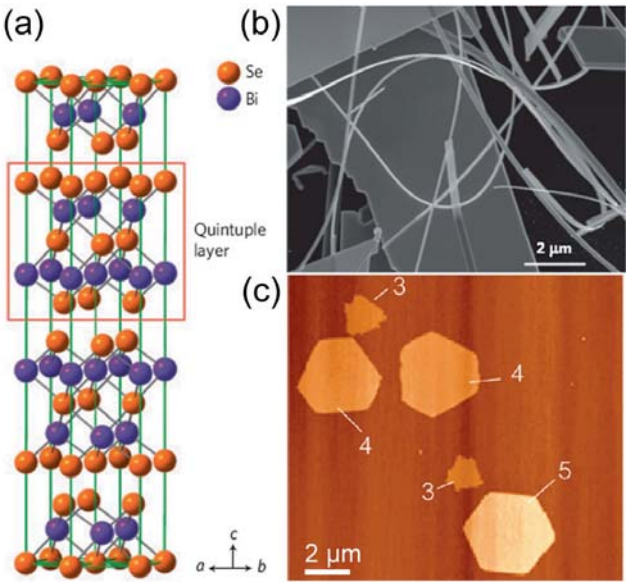

Figure 2 (online color at: www.pss-rapid.com) (a) Layered crystal structure of Bi_2Se_3 where the covalently bonded Se–Bi–Se–Bi–Se atomic planes make a ~1 nm thick quintuple layer. Neighboring quintuple layers interact by van der Waals force. (b) Scanning electron microscope (SEM) image of Bi_2Se_3 nanoribbons grown via VLS method. (c) AFM image of Bi_2Te_3 nanoplates grown via VS mechanism. The numbers indicate the nanoplate thickness in nanometers. (a) and (b) Reprinted by permission from Macmillan Publishers Ltd., Ref. [58], copyright (2010). (c) Reprinted with permission from Ref. [42], copyright (2010), American Chemical Society.

thin TI flakes are cleaved from the bulk by an adhesive tape. This is possible because Bi_2Se_3, Bi_2Te_3, and Sb_2Te_3, the first three binary chalcogenides which were identified as 3D TIs, are layered structure in which adjacent layers are held together by the weak van der Waals interactions (Fig. 2(a)). Although simple, the mechanical exfoliation method poses a few issues such as potentially damaging the crystal during cleavage, providing irregularly shaped flakes with rough edges after exfoliation, and low yield. These can increase scattering, thus affecting transport measurements significantly. Alternatively, an atomic force microscope (AFM) tip can be used to exfoliate part of TI nanoribbons to obtain ultrathin TI nanomaterials [57]. This method creates smooth surfaces but the yield is low.

In contrast, VLS and VS growth methods produce large quantities of single-crystalline nanostructures with well-defined morphology. Bi_2Se_3, Bi_2Te_3, and Sb_2Te_3 have been synthesized into nanoribbons using metal growth catalysts [41, 59] and nanoplates in the absence of metal catalysts [42, 59]. Figure 2(b) and (c) show VLS-grown Bi_2Se_3 nanoribbons and VS-grown Bi_2Te_3 nanoplates, respectively. Few-layer thick, large Bi_2Se_3 sheets expanding several tens of microns have also been synthesized on various substrates such as graphite and mica [51]. Crystal quality of these nanostructures is high, with negligible defect densities. In the VLS growth case, strain effects due to the growth substrate, an issue for thin-film expitaxy growth techniques such as MBE, is also eliminated as the nanostructures shoot off from the substrate.

Tunable chemical compositions such as $(Sb_xBi_{1-x})_2Te_3$ nanoplates [60] and $Bi_2(Se_xTe_{1-x})_3$ nanoribbons and nanoplates [61] and various dopants such as Sb and Fe [62, 63] have been reported in TI nanostructures using the VLS and VS methods. The wide tuning range of the composition and the dopant concentration make it possible to engineer the band structure of the TIs such that TI surface states are the dominant feature in transport measurements.

4.2 Chemical synthesis Chemical synthesis of TI nanomaterials, primarily the noncentro-symmetric zinc-blende HgTe-type family and the hexagonal centro-symmetric Bi_2Se_3 family of compounds, has been achieved with a diverse set of methods: colloidal [64–66], solvothermal [67–69], hydrothermal co-reduction [70], mechano-chemical [71, 72], photochemical [73], galvanic displacement [74], and a microwave-assisted synthesis [75].

Chemical methods offer significant practical advantages compared to the bulk synthesis and the physical nanomaterial synthesis. The synthesis time is relatively short requiring only a few minutes to a day and synthesis temperature can be fairly low (<300 °C). With these mild synthesis requirements, significant control both in morphology and chemical modification of the surface can be achieved, which will be useful in designing device architectures ideal for enhancing the surface effects. Extensive morphological control of TI nanostructures has been demonstrated using synthetic chemistry, such as nanoribbons [75], nanorods [65], nanowires [66], nanotubes [74], nanoplates [77], nanorings [75], nanospheres [78], and quantum dots [79]. The crystalline quality of the chemically synthesized TI nanomaterials is high (Fig. 3(a)–(c)), as evidenced in the transport studies of the solvothermally grown B_2Te_3 nanoribbons [76]. The Bi_2Te_3 nanoribbons in this study were synthesized by low temperature reduction at <250 °C combining ethylene diamene tetraacetic acid (EDTA), polyvinylpyrrollidone (PVP), bismuth oxide, and tellurium in a reducing solvent, ethylene glycol. This synthesis method allows *in-situ* or *ex-situ* chemical doping as demonstrated in sodium doping in Bi_2Te_3 [80], and *in-situ* surface capping/modification layer to protect the TI surface states from environmental degradation such as oxidation. Figure 3(d) and (e) show Sb_2Te_3 nanoplates synthesized by a solvothermal approach.

Wet, chemical exfoliation is another way to acheive TI nanostructures from bulk materials. Similar to the scotch tape method, it exploits the weak van der Waals interactions to separate neighboring layers. Large quantities of thin TI films can be achieved in this way. Single-layer metal chalcogenide flakes, such as MoS_2, WS_2, $MoSe_2$, and Bi_2Te_3, have been obtained by chemical exfoliation using common solvents [81].

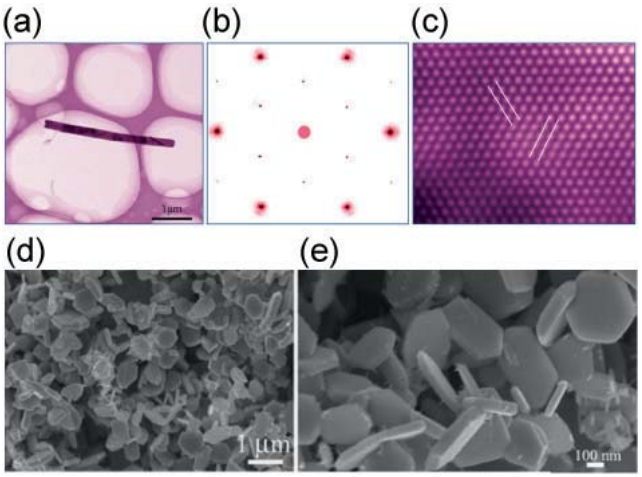

Figure 3 (online color at: www.pss-rapid.com) (a) Solvothermally synthesized Bi_2Te_3 nanoribbon. Electron diffraction pattern (b) and high-resolution transmission electron microscope image (c) show single crystalline material. (d) and (e) SEM images of Sb_2Te_3 nanoplates synthesized by a solvothermal approach. (a)–(c) Reprinted by permission from Macmillan Publishers Ltd., Ref. [76], copyright (2011). (d) and (e) Reprinted with permission from Ref. [69], copyright (2005), American Chemical Society.

Presently, the electronic properties of chemically synthesized TI nanostructures have not been fully investigated. The mobility of the TI surface states in these TI nanomaterials are expected to be high, as evidenced by the SdH and AB oscillations observed in solvothermally grown Bi_2Te_3 nanoribbons [76]. Thus, careful transport measurements on chemically synthesized TI nanomaterials are encouraged. Given the wide morphological control and compositional tunability available in the chemical synthesis methods, future investigation in chemically synthesized TIs will become increasingly important.

5 Notable experimental results in TI nanostructures In this section, we review transport measurements on the TI nanostructures. Results similar to the bulk and thin film studies have been obtained in the TI nanostructures. For example, the presence of the TI surface states in VS-grown Bi_2Se_3 nanosheets has been confirmed by ARPES (Fig. 4) [51], and weak anti-localization has also been reported in various flakes, nanoribbons and nanoplates [42, 61, 82]. Observations of SdH oscillations are also reported [50, 80, 83], but more careful studies are necessary to confirm their surface origin unambiguously. For example, SdH oscillations from bulk carriers in heavily-doped Bi_2Se_3 flakes were shown to be 2D-like [84]. Crossover from weak anti-localization to localization was also observed in Fe-doped Bi_2Se_3 nanoribbons [63]. The spin-momentum locking property of the TI surface electrons has been probed by optically pumping the TI surface electrons with circularly polarized light and measuring the subsequent current direction [85].

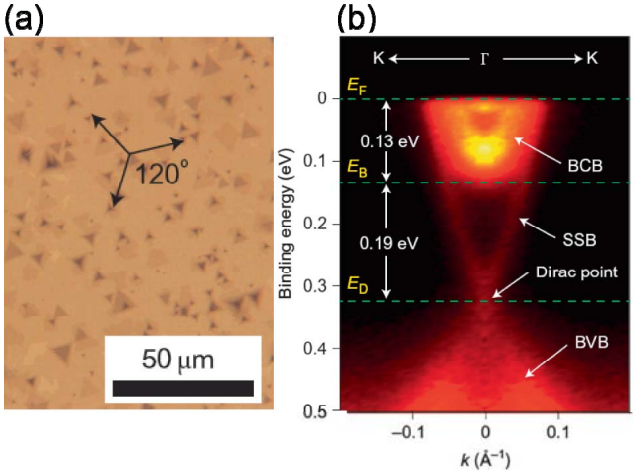

Figure 4 (online color at: www.pss-rapid.com) (a) Optical microscope image of large-area, few-layer Bi_2Se_3 nanosheets grown on a mica substrate. (b) ARPES-measured band structure of Bi_2Se_3 nanosheets. The surface state band (SSB) is clearly visible. Reprinted with permission from Macmillan Publishers Ltd., Ref. [51], copyright (2012).

5.1 Aharonov–Bohm oscillations The unique advantage that TI nanostructures offer is their well-defined nanoscale morphology, ideal for interference-type experi-

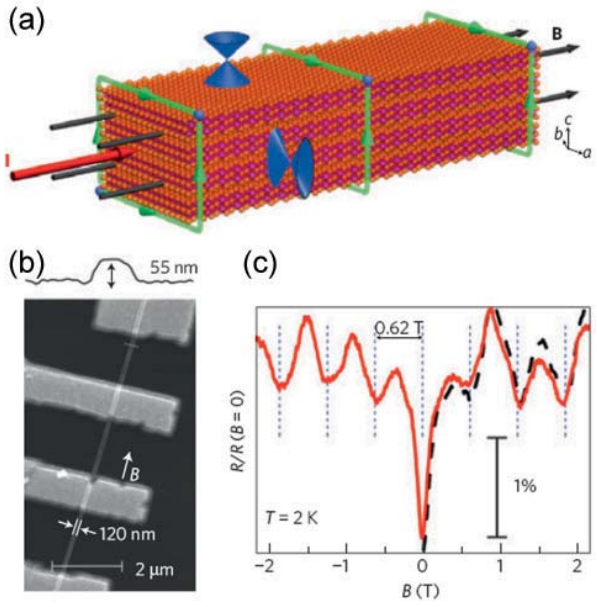

Figure 5 (online color at: www.pss-rapid.com) (a) Schematic diagram of the surface electrons travelling on the surface of the Bi_2Se_3 nanoribbon, indicated by the green paths, while the magnetic field (black arrows) threads through the nanoribbon. (b) SEM image of the Bi_2Se_3 nanoribbon device with four Ti/Au contacts. The height profile measured by AFM indicates that the ribbon is 55 nm thick. (c) Normalized magnetoresistance as a function of the parallel magnetic field at 2 K. The periodic oscillations observed in the resistance trace are AB oscillations. This figure is reprinted with permission from Macmillan Publishers Ltd., Ref. [58], copyright (2010).

ments for the TI surface states. One such interference is Aharonov–Bohm (AB) oscillations [48, 49], which are periodic oscillations in conductance arising from constructively and destructively interfering electrons travelling in a well-defined path in the presence of magnetic flux. The magnetic fields thread through the cross-section of the well-defined path (Fig. 5(a)).

So far, only narrow nanoribbons with widths of ~100 nm and smooth surfaces show AB oscillations. AB oscillations were observed in VLS grown Bi_2Se_3 nanoribbons (Fig. 5) [58] and chemically synthesized Bi_2Te_3 nanoribbons [76]. Both of these synthesis techniques do not require high vacuum apparatus or precise control of the growth conditions. Thus, growth techniques do not appear to affect the intrinsic TI properties. Mechanically exfoliated flakes will not exhibit AB oscillations due to their irregular shapes which will destroy coherence phases. Nor will bulk TI crystals show AB oscillations as the cross-section of bulk TI crystals is macroscopic, much larger than the phase coherent length of the TI surface states.

5.2 Fermi level tuning Another transport advantage TI nanostructures offer is effective field-effect gating to tune the Fermi level, made possible by the fact that these nanostructures are only tens of nanometers thick or thinner. Charge doping using Sb and other dopants has proven effective in reducing the bulk carriers in nanostructures [62, 80], similar to the bulk crystals. Still, complete elimination of bulk residual carriers purely by doping continues to be very difficult. Thus, Fermi level control by field-effect gating is necessary to eliminate residual bulk carriers, resulting in transport from the TI surface state only. For effective gating, thin films and nanostructures are promising, and several studies successfully demonstrated ambipolar behavior in thin Bi_2Te_3, Bi_2Se_3, and $(Sb_xBi_{1-x})_2Te_3$ nanostructures (Fig. 6) [54, 60, 62, 80]. Ionic liquid gating has also shown to be effective in controlling the Fermi level [39, 86].

Effective tuning of the Fermi level to reduce the bulk residual carriers has also been demonstrated in MBE-grown thin films. For example, transition from n- to p-type via composition tuning has been shown in MBE-grown $(Sb_xBi_{1-x})_2Te_3$ thin films [38]. However, in the absence that proximity effects are desired, nanomaterials may be desirable over thin films. This is because they can be deposited on any substrates without building strains, which can be problematic in thin-film growth techniques that usually require stringent lattice matching between the TI materials and the growth substrates. Strains may play a role in reducing the mobility of the TI surface electron. Only recently were SdH oscillations observed in MBE-grown Bi_2Se_3 thin film grown expitaxially on sapphire (0001) substrates [28].

5.3 Proximity effects Proximity effects, which arise when the TI surface states are in close proximity with other strongly correlated electronic states, are hotly pursued. One such system is a Josephson junction where the TI is sandwiched between two closely-placed superconducting leads [87, 88], producing a 'topological superconductor'. An elusive quasiparticle, called the Majorana fermion [89, 90], is expected to arise in the proposed set-up. A schematic using Bi_2Se_3 as a TI is shown in Fig. 7(a) and a real device in Fig. 7(b).

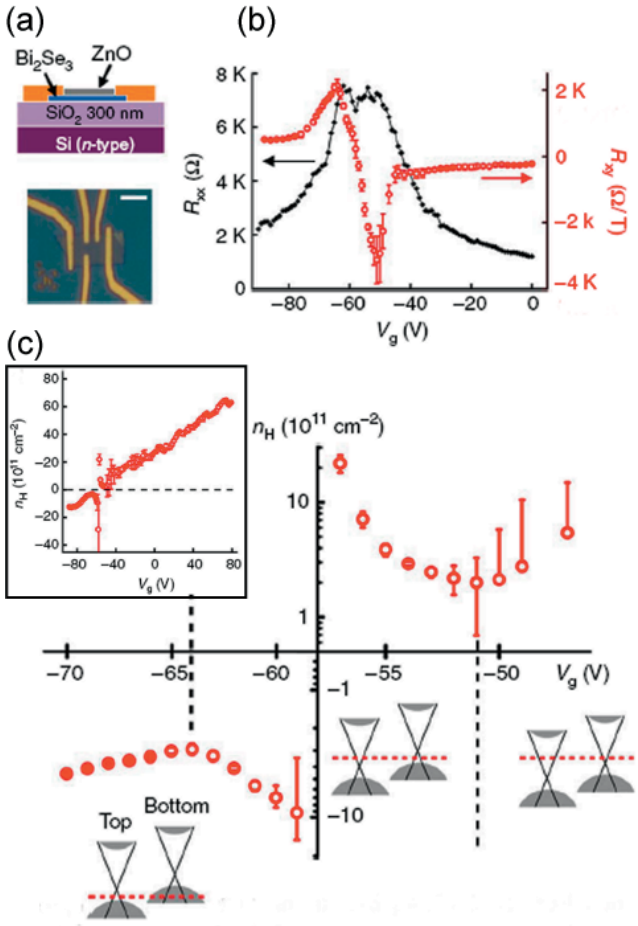

Figure 6 (online color at: www.pss-rapid.com) (a) Schematic diagram of the Sb-doped Bi_2Se_3 nanoribbon device, capped with a protection layer of sputtered ZnO. (b) Ambipolar gating effect has been demonstrated as evidenced by the peak in the resistance (black curve) and the sign change in the Hall resistance (red curve) as a function of the back gate voltage. (c) Carrier density of ~2×10^{11} cm^{-2} has been obtained, which indicates surface state only transport with the Fermi level of the top surface located ~40 meV above the Dirac point. Reprinted by permission from Macmillan Publishers Ltd., Ref. [62], copyright (2012).

Several groups have reported transport results on such set up using topological insulator nanostructures and superconducting leads [26, 87, 91–94]. Some report transport results that resemble typical characteristics of conventional Josephson junctions; this may be due to the residual bulk carriers in TIs. Work by Williams et al. (Fig. 7) [92] shows two distinct departures from a conventional Josephson junction, which they attribute as signature of Majorana fermions in 1D channel. More careful studies are ongoing.

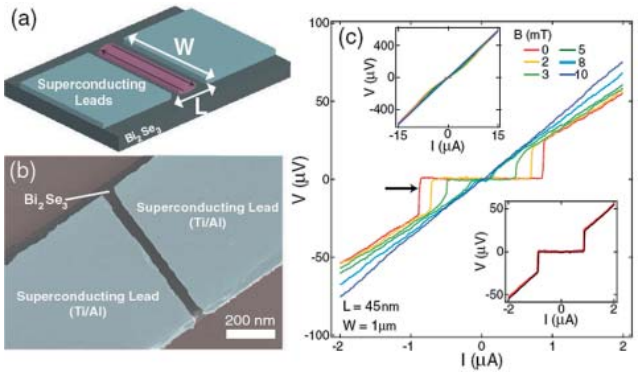

Figure 7 (online color at: www.pss-rapid.com) (a) Schematic diagram of the topological insulator Josephson junction. Two superconducting contacts are closely patterned on top of Bi_2Se_3. In between the contacts is a one-dimensional wire of Majorana fermions. (b) SEM image of a device. (c) V vs. I traces of a device at different magnetic fields at 12 mK. At $V = 0$, a supercurrent flows when current (I) is below a critical current. As the perpendicular magnetic field increases, the critical current systematically decreases. Reprinted with permission from Ref. [92]. Copyright (2012) by American Physical Society.

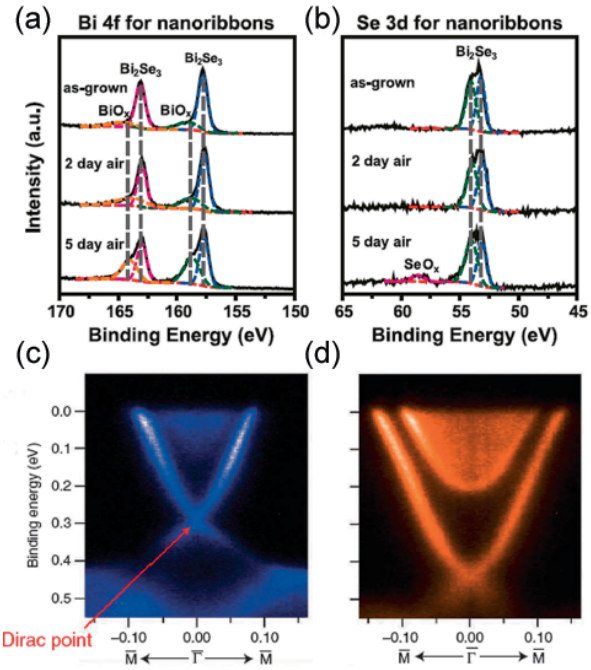

Figure 8 (online color at: www.pss-rapid.com) X-ray photoemission spectroscopy of Bi-edge (a) and Se-edge (b) from Bi_2Se_3 nanoribbons shows significant surface oxidation over time. (c) Band structure of freshly cleaved Bi_2Se_3 surface measured by AR-PES. (d) Band structure of Bi_2Se_3 after left in vacuum for three hours. The Dirac point has shifted down and the sharp rim around the conduction band edge indicates emergence of the 2D electron gas. (a, b) Reproduced with permission from Ref. [98], copyright (2011), American Chemical Society. (c, d) Reprinted with permission from Macmillan Publishers Ltd., Ref. [100], copyright (2010).

Simultaneously, other nanostructures with strong spin–orbit coupling such as InSb nanowires are pursued for Majorana fermion studies [47, 95].

Another proximity effect actively under investigation is a TI material in contact with a ferromagnetic insulator possessing magnetic moments perpendicular to the interface. A surface band gap is expected at the interface [32, 96], which can lead to truly dissipationless transport and transistors using the TI surface state as the information-carrying bit. Mn-doped $Bi_2Te_{3-y}Se_y$ flakes obtained from bulk crystals suggest 1D edge-state transport of the TI surface electrons on the magnetic domain wall [97]. For the ferromagnetic proximity effect, thin film epitaxy of TI films grown directly on ferromagnetically insulating substrates have an advantage over TI nanomaterials because the coupling strength for the proximity effect is expected to be stronger as compared to TI nanomaterials placed on top of ferromagnetic insulators. However, heterostructure nanostructures consisting of the TI layers and the ferromagnetically insulating layers may ultimately be realized to increase the proximity effects.

6 Nanomaterial solutions to degrading surface states The current challenge facing the progress of studying the TI surface states is the fast degradation of the surface states when the TIs are exposed to air. Surface oxidation and other adatoms appear to reduce the mobility of the surface states dramatically, and to populate additional electron carriers that dominate transport (Fig. 8) [98, 99]. Charge fluctuations induced by charged impurities on the surface of the TI material also lead to fluctuations in the position of the Dirac point. Moreover, 2D electron gases also form when the TIs are exposed to air (Fig. 8(c) and (d)), complicating the study of the true topological surface state [100, 101].

Ex-situ coating of nanostructures achieved partial success in eliminating unwanted carriers due to 'environmental doping'. ZnO sputter-coating of Bi_2Se_3 nanoribbons after cleaning the nanoribbon surface by soft Ar plasma-etching showed the lowest carrier density achieved thus far by field-effect gating (Fig. 6) [62]. In this system, all the carriers were shown to arise from the surface states with the Fermi level close to Dirac point. However, mobility of the TI surface states was low, which could partially be attributed to the unavoidable damage induced during soft etching and subsequent ZnO sputtering. Thus, *in-situ* coating appears essential. *In-situ* coating of bulk crystals is problematic as the surface signal in bulk will be very small. Mechanical exfoliation to obtain nanoflakes from bulk crystals is incompatible with *in-situ* coating. In thin films, *in-situ* coating such as Se coating and Al passivation [102] was done, but only recently has thin film quality improved to show clear SdH oscillations [28]. As mentioned previously, substrate strain effects that likely degrade the mobility of the surface states should be addressed in thin film growths.

In nanomaterial synthesis, *in-situ* coating can be easily integrated with growth. In physical synthesis, after the nanomaterial growth, vapor of the coating layer can be introduced for a conformal coating of the protection layer. In chemical synthesis, surface ligands, such as PVP and EDTA, can effectively prevent degradation of the sample from the environmental exposure. In addition to serving as a protection layer, surface functionalization is possible during the chemical synthesis, by utilizing functional ligands as a coating layer. A self-assembled magnetic molecular layer has recently been shown to induce magnetic moments in thin gold film [103], which attests to the strength of surface modification.

7 Future experiments using TI nanostructures Once the surface degradation problem is overcome, mobility of the TI surface states is expected to be high to observe clear quantum oscillations. Much clearer SdH oscillations as a function of the magnetic field direction and the field-effect gating voltage should be demonstrated in TI nanomaterials. Careful studies on AB oscillations should be carried out. It has been pointed out that the phase of the AB oscillations observed in the VLS-grown Bi_2Se_3 nanoribbons [58, 104] indicates TI surface electrons in diffusive regime [104]. Measuring the phase in the ballistic regime is crucial to show that the AB oscillations are truly coming from the TI surface states. Proximity effects, such as TIs in contact with superconductors and ferromagnetic insulators, should be studied more carefully. These fundamental studies will lay ground for future applications such as dissipationless interconnects, enhanced thermoelectric materials, and TI transistors.

8 Material perspectives: going beyond topological insulators Nanometerials synthesis offers morphological, electronic, and chemical control, ultimately culminating in the ability to specifically engineer structures with desirable TI properties at the nanoscale [11, 41, 42, 60]. Current and future thrusts in TIs are to (i) create heterostructures with other materials such as superconductors and ferromagnetic insulators [32, 33, 36, 96], (ii) use chemical means for doping and surface modifications [80], and (iii) use chemical intercalation for wider tunability of the materials properties [105, 106]. Heterostructures of varying topological insulator layers can be used to alter the surface states or to take advantage of new material behavior. For example, nanoscale heterostructures with superconductors can be used to take advantage of the Majorana fermions. Heterostructures of TI materials with ferromagnetic materials can be used for spintronics.

Chemical doping on the nanoscale has revolutionized the field of graphene as a method to open up a band-gap and to adjust the electronic properties. These methods are equally relevant to TIs as a means to tune the electronic and structural properties, thereby tuning the TI behavior on an atomic level. Reactions such as chemical exchange can also be used to replace single atoms, directly manipulating the TI behavior for desired properties. Since most of the currently studied TI materials, such as the Bi_2Se_3 class of materials, are layered materials and possess van der Waals gaps, chemical intercalation is another methodology to atomically tune the electronic and structural behavior of the TIs. Indeed, many examples exist, such as copper intercalation into Bi_2Se_3 culminating in superconductivity [33, 34] and possibly topological superconductivity.

Like all crystalline materials, TI materials are not immune to defects, dislocations, and impurities. Sometimes, defects, such as screw dislocations, can be used for growth of TI materials. For example, MBE growth of TI chalcogenides on substrates such as GaAs and Si initiates from a dislocation [107, 108]. Screw dislocation-driven growth of 2D ZnO nanoplates by chemical synthesis has also been observed [109]. Similar growth mechanism may be possible in TI nanomaterials. To date, no obvious consequences of structural defects on the topological property have been observed experimentally, post-growth. Theoretically, a screw disclocation in TI has been predicted to accommodate a pair of protected 1D helical modes [110, 111]. Engineering of dislocations in TI nanostructures is thus needed to test the theoretical predictions.

9 Conclusion The progress in TI field has been remarkable. With further advancements in nanomaterial synthesis and *in-situ* coatings, future experiments may reveal the fundamental nature of topological protection in detail. A myriad of possibilities waits to be pursued in nanostructures such as intercalation in TI nanomaterials and exfoliation/restacking of TI layers and other thin layers. These avenues will enable us to tune the materials properties much more broadly than any conventional methods.

The technological future of TIs appears bright. Nanoscale TI materials may find use in a variety of applications including new interconnects in electronic devices, transistor memory devices, high sensitivity magnetic sensors, energy efficient electronics, new high-speed infrared detectors, and new thermoelectric devices [112]. Dissipationless TIs may even revolutionize the power grid [96]. Ultimately, as TIs achieve truly dissipationless transport and find increasing involvement in full-scale electronics, it will be necessary to scale up synthesis of these materials for which chemical means will need to be employed. It will be equally important to develop new ways of protecting the surface states from long-term degradation for long-lifetime devices and to allow TI behavior to exist above cryogenic temperatures.

Acknowledgements Authors acknowledge support from a DARPA MESO project (No. N66001-11-1-4105).

References

[1] C. L. Kane and E. J. Mele, Phys. Rev. Lett. **95**, 146802 (2005).

[2] B. A. Bernevig, T. L. Hughes, and S.-C. Zhang, Science **314**, 1757 (2006).

[3] M. Konig, S. Wiedmann, C. Brune, A. Roth, H. Buhmann, L. W. Molenkamp, X.-L. Qi, and S.-C. Zhang, Science **318**, 766 (2007).
[4] M. Z. Hasan and C. L. Kane, Rev. Mod. Phys. **82**, 3045 (2010).
[5] X.-L. Qi and S.-C. Zhang, Rev. Mod. Phys. **83**, 1057 (2011).
[6] K. v. Klitzing, G. Dorda, and M. Pepper, Phys. Rev. Lett. **45**, 494 (1980).
[7] D. J. Thouless, M. Kohmoto, M. P. Nightingale, and M. den Nijs, Phys. Rev. Lett. **49**, 405 (1982).
[8] L. Fu, C. L. Kane, and E. J. Mele, Phys. Rev. Lett. **98**, 106803 (2007).
[9] H. Zhang, C.-X. Liu, X.-L. Qi, X. Dai, Z. Fang, and S.-C. Zhang, Nature Phys. **5**, 438 (2009).
[10] J. E. Moore, Nature **464**, 194 (2010).
[11] D. Kong and Y. Cui, Nature Chem. **3**, 845 (2011).
[12] D. Hsieh, D. Qian, L. Wray, Y. Xia, Y. S. Hor, R. J. Cava, and M. Z. Hasan, Nature **452**, 970 (2008).
[13] Y. Xia, D. Qian, D. Hsieh, L. Wray, A. Pal, H. Lin, A. Bansil, D. Grauer, Y. S. Hor, R. J. Cava, and M. Z. Hasan, Nature Phys. **5**, 398 (2009).
[14] Y. L. Chen, J. G. Analytis, J. H. Chu, Z. K. Liu, S. K. Mo, X. L. Qi, H. J. Zhang, D. H. Lu, X. Dai, Z. Fang, S. C. Zhang, I. R. Fisher, Z. Hussain, and Z. X. Shen, Science **325**, 178 (2009).
[15] D. Hsieh, Y. Xia, D. Qian, L. Wray, J. H. Dil, F. Meier, J. Osterwalder, L. Patthey, J. G. Checkelsky, N. P. Ong, A. V. Fedorov, H. Lin, A. Bansil, D. Grauer, Y. S. Hor, R. J. Cava, and M. Z. Hasan, Nature **460**, 1101 (2009).
[16] D. Hsieh, Y. Xia, L. Wray, D. Qian, A. Pal, J. H. Dil, J. Osterwalder, F. Meier, G. Bihlmayer, C. L. Kane, Y. S. Hor, R. J. Cava, and M. Z. Hasan, Science **323**, 919 (2009).
[17] P. Cheng, C. Song, T. Zhang, Y. Zhang, Y. Wang, J.-F. Jia, J. Wang, Y. Wang, B.-F. Zhu, X. Chen, X. Ma, K. He, L. Wang, X. Dai, Z. Fang, X. Xie, X.-L. Qi, C.-X. Liu, S.-C. Zhang, and Q.-K. Xue, Phys. Rev. Lett. **105**, 076801 (2010).
[18] P. Roushan, J. Seo, C. V. Parker, Y. S. Hor, D. Hsieh, D. Qian, A. Richardella, M. Z. Hasan, R. J. Cava, and A. Yazdani, Nature **460**, 1106 (2009).
[19] Y. Zhang, K. He, C.-Z. Chang, C.-L. Song, L.-L. Wang, X. Chen, J.-F. Jia, Z. Fang, X. Dai, W.-Y. Shan, S.-Q. Shen, Q. Niu, X.-L. Qi, S.-C. Zhang, X.-C. Ma, and Q.-K. Xue, Nature Phys. **6**, 584 (2010).
[20] Y. L. Chen, J. H. Chu, J. G. Analytis, Z. K. Liu, K. Igarashi, H.-H. Kuo, X. L. Qi, S. K. Mo, R. G. Moore, D. H. Lu, M. Hashimoto, T. Sasagawa, S. C. Zhang, I. R. Fisher, Z. Hussain, and Z. X. Shen, Science **329**, 659 (2010).
[21] S.-Y. Xu, M. Neupane, C. Liu, D. Zhang, A. Richardella, L. Andrew Wray, N. Alidoust, M. Leandersson, T. Balasubramanian, J. Sanchez-Barriga, O. Rader, G. Landolt, B. Slomski, J. Hugo Dil, J. Osterwalder, T.-R. Chang, H.-T. Jeng, H. Lin, A. Bansil, N. Samarth, and M. Zahid Hasan, Nature Phys. **8**, 616 (2012).
[22] D.-X. Qu, Y. S. Hor, J. Xiong, R. J. Cava, and N. P. Ong, Science **329**, 821 (2010).
[23] J. G. Analytis, R. D. McDonald, S. C. Riggs, J.-H. Chu, G. S. Boebinger, and I. R. Fisher, Nature Phys. **6**, 960 (2010).
[24] Z. Ren, A. A. Taskin, S. Sasaki, K. Segawa, and Y. Ando, Phys. Rev. B **82**, 241306 (2010).
[25] J. Xiong, A. C. Petersen, D. Qu, Y. S. Hor, R. J. Cava, and N. P. Ong, Physica E **44**, 917 (2012).
[26] B. Sacépé, J. B. Oostinga, J. Li, A. Ubaldini, N. J. G. Couto, E. Giannini, and A. F. Morpurgo, Nature Commun. **2**, 575 (2011).
[27] S. Hikami, A. I. Larkin, and Y. Nagaoka, Prog. Theor. Phys. **63**, 707 (1980).
[28] A. A. Taskin, S. Sasaki, K. Segawa, and Y. Ando, Phys. Rev. Lett. **109**, 066803 (2012).
[29] M. Liu, J. Zhang, C.-Z. Chang, Z. Zhang, X. Feng, K. Li, K. He, L.-l. Wang, X. Chen, X. Dai, Z. Fang, Q.-K. Xue, X. Ma, and Y. Wang, Phys. Rev. Lett. **108**, 036805 (2012).
[30] H.-T. He, G. Wang, T. Zhang, I.-K. Sou, G. K. L. Wong, J.-N. Wang, H.-Z. Lu, S.-Q. Shen, and F.-C. Zhang, Phys. Rev. Lett. **106**, 166805 (2011).
[31] C.-Z. Chang, J. Zhang, M. Liu, Z. Zhang, X. Feng, K. Li, L. Wang, X. Chen, X. Dai, Z. Fang, X. L. Qi, S. C. Zhang, Y. Wang, K. He, X. Ma, and Q. Xue, arXiv:1108.4754v1 (2011).
[32] R. Yu, W. Zhang, H.-J. Zhang, S.-C. Zhang, X. Dai, and Z. Fang, Science **329**, 61 (2010).
[33] Y. S. Hor, A. J. Williams, J. G. Checkelsky, P. Roushan, J. Seo, Q. Xu, H. W. Zandbergen, A. Yazdani, N. P. Ong, and R. J. Cava, Phys. Rev. Lett. **104**, 057001 (2010).
[34] S. Sasaki, M. Kriener, K. Segawa, K. Yada, Y. Tanaka, M. Sato, and Y. Ando, Phys. Rev. Lett. **107**, 217001 (2011).
[35] M. Kriener, K. Segawa, Z. Ren, S. Sasaki, S. Wada, S. Kuwabata, and Y. Ando, Phys. Rev. B **84**, 054513 (2011).
[36] M.-X. Wang, C. Liu, J.-P. Xu, F. Yang, L. Miao, M.-Y. Yao, C. L. Gao, C. Shen, X. Ma, X. Chen, Z.-A. Xu, Y. Liu, S.-C. Zhang, D. Qian, J.-F. Jia, and Q.-K. Xue, Science **336**, 52 (2012).
[37] Y. S. Hor, A. Richardella, P. Roushan, Y. Xia, J. G. Checkelsky, A. Yazdani, M. Z. Hasan, N. P. Ong, and R. J. Cava, Phys. Rev. B **79**, 195208 (2009).
[38] J. Zhang, C.-Z. Chang, Z. Zhang, J. Wen, X. Feng, K. Li, M. Liu, K. He, L. Wang, X. Chen, Q.-K. Xue, X. Ma, and Y. Wang, Nature Commun. **2**, 574 (2011).
[39] H. Yuan, H. Liu, H. Shimotani, H. Guo, M. Chen, Q. Xue, and Y. Iwasa, Nano Lett. **11**, 2601 (2011).
[40] D. Teweldebrhan, V. Goyal, and A. A. Balandin, Nano Lett. **10**, 1209 (2010).
[41] D. Kong, J. C. Randel, H. Peng, J. J. Cha, S. Meister, K. Lai, Y. L. Chen, Z. X. Shen, H. C. Manoharan, and Y. Cui, Nano Lett. **10**, 329 (2010).
[42] D. Kong, W. Dang, J. J. Cha, H. Li, S. Meister, H. Peng, Z. Liu, and Y. Cui, Nano Lett. **10**, 2245 (2010).
[43] W. Lu and C. M. Lieber, J. Phys. D: Appl. Phys. **39**, R387 (2006).
[44] M. Law, J. Goldberger, and P. Yang, Annu. Rev. Mater. Res. **34**, 83 (2004).
[45] Y. Hu, H. O. H. Churchill, D. J. Reilly, J. Xiang, C. M. Lieber, and C. M. Marcus, Nature Nano. **2**, 622 (2007).
[46] C. Thelander, M. T. Björk, M. W. Larsson, A. E. Hansen, L. R. Wallenberg, and L. Samuelson, Solid State Commun. **131**, 573 (2004).
[47] V. Mourik, K. Zuo, S. M. Frolov, S. R. Plissard, E. P. A. M. Bakkers, and L. P. Kouwenhoven, Science **336**, 1003 (2012).
[48] Y. Aharonov and D. Bohm, Phys. Rev. **115**, 485 (1959).

[49] R. A. Webb, S. Washburn, C. P. Umbach, and R. B. Laibowitz, Phys. Rev. Lett. **54**, 2696 (1985).
[50] H. Tang, D. Liang, R. L. J. Qiu, and X. P. A. Gao, ACS Nano **5**, 7510 (2011).
[51] H. Peng, W. Dang, J. Cao, Y. Chen, D. Wu, W. Zheng, H. Li, Z.-X. Shen, and Z. Liu, Nature Chem. **4**, 281 (2012).
[52] H. Guolin, Q. Xiang, L. Yundan, H. Zongyu, L. Hongxing, H. Kai, L. Jun, Y. Liwen, and Z. Jianxin, J. Appl. Phys. **111**, 114312 (2012).
[53] L. D. Alegria, M. D. Schroer, A. Chatterjee, G. R. Poirier, M. Pretko, S. K. Patel, and J. R. Petta, Nano Lett. **12**, 4711 (2012).
[54] H. Steinberg, D. R. Gardner, Y. S. Lee, and P. Jarillo-Herrero, Nano Lett. **10**, 5032 (2010).
[55] K. S. Novoselov, A. K. Geim, S. V. Morozov, D. Jiang, Y. Zhang, S. V. Dubonos, I. V. Grigorieva, and A. A. Firsov, Science **306**, 666 (2004).
[56] K. S. Novoselov, D. Jiang, F. Schedin, T. J. Booth, V. V. Khotkevich, S. V. Morozov, and A. K. Geim, Proc. Natl. Acad. Sci. USA **102**, 10451 (2005).
[57] S. S. Hong, W. Kundhikanjana, J. J. Cha, K. Lai, D. Kong, S. Meister, M. A. Kelly, Z.-X. Shen, and Y. Cui, Nano Lett. **10**, 3118 (2010).
[58] H. Peng, K. Lai, D. Kong, S. Meister, Y. Chen, X.-L. Qi, S.-C. Zhang, Z.-X. Shen, and Y. Cui, Nature Mater. **9**, 225 (2010).
[59] J. S. Lee, S. Brittman, D. Yu, and H. Park, J. Am. Chem. Soc. **130**, 6252 (2008).
[60] D. Kong, Y. Chen, J. J. Cha, Q. Zhang, J. G. Analytis, K. Lai, Z. Liu, S. S. Hong, K. J. Koski, S.-K. Mo, Z. Hussain, I. R. Fisher, Z.-X. Shen, and Y. Cui, Nature Nano. **6**, 705 (2011).
[61] J. J. Cha, D. Kong, S.-S. Hong, J. G. Analytis, K. Lai, and Y. Cui, Nano Lett. **12**, 1107 (2012).
[62] S. S. Hong, J. J. Cha, D. Kong, and Y. Cui, Nature Commun. **3**, 757 (2012).
[63] J. J. Cha, M. Claassen, D. Kong, S. S. Hong, K. J. Koski, X.-L. Qi, and Y. Cui, Nano Lett. **12**, 4355 (2012).
[64] A. Rogach, S. V. Kershaw, M. Burt, M. T. Harrison, A. Kornowski, A. Eychmüller, and H. Weller, Adv. Mater. **11**, 552 (1999).
[65] H. Yu, P. C. Gibbons, and W. E. Buhro, J. Mater. Chem. **14**, 595 (2004).
[66] A. Purkayastha, F. Lupo, S. Kim, T. Borca-Tasciuc, and G. Ramanath, Adv. Mater. **18**, 496 (2006).
[67] S. K. Batabyal, C. Basu, A. R. Das, and G. S. Sanyal, Mater. Lett. **60**, 2582 (2006).
[68] Y. Deng, C.-W. Cui, N.-L. Zhang, T.-H. Ji, Q.-L. Yang, and L. Guo, Solid State Commun. **138**, 111 (2006).
[69] W. Wang, B. Poudel, J. Yang, D. Z. Wang, and Z. F. Ren, J. Am. Chem. Soc. **127**, 13792 (2005).
[70] H. Cui, H. Liu, X. Li, J. Wang, F. Han, X. Zhang, and R. I. Boughton, J. Solid State Chem. **177**, 4001 (2004).
[71] E. Klose and R. Blachnik, Thermochim. Acta **375**, 147 (2001).
[72] K. Kim, K. Kim, and G. Ha, Electron. Mater. Lett. **6**, 177 (2010).
[73] S. Xu, W.-b. Zhao, J.-M. Hong, J.-J. Zhu, and H.-Y. Chen, Mater. Lett. **59**, 319 (2005).
[74] F. Xiao, B. Yoo, K. H. Lee, and N. V. Myung, J. Am. Chem. Soc. **129**, 10068 (2007).
[75] Y. Jiang and Y.-J. Zhu, J. Cryst. Growth **306**, 351 (2007).
[76] F. Xiu, L. He, Y. Wang, L. Cheng, L.-T. Chang, M. Lang, G. Huang, X. Kou, Y. Zhou, X. Jiang, Z. Chen, J. Zou, A. Shailos, and K. L. Wang, Nature Nano. **6**, 216 (2011).
[77] Y. Deng, X.-S. Zhou, G.-D. Wei, J. Liu, C.-W. Nan, and S.-J. Zhao, J. Phys. Chem. Solids **63**, 2119 (2002).
[78] O. Palchik, R. Kerner, Z. Zhu, and A. Gedanken, J. Solid State Chem. **154**, 530 (2000).
[79] S. Keuleyan, E. Lhuillier, and P. Guyot-Sionnest, J. Am. Chem. Soc. **133**, 16422 (2011).
[80] Y. Wang, F. Xiu, L. Cheng, L. He, M. Lang, J. Tang, X. Kou, X. Yu, X. Jiang, Z. Chen, J. Zou, and K. L. Wang, Nano Lett. **12**, 1170 (2012).
[81] J. N. Coleman, M. Lotya, A. O'Neill, S. D. Bergin, P. J. King, U. Khan, K. Young, A. Gaucher, S. De, R. J. Smith, I. V. Shvets, S. K. Arora, G. Stanton, H.-Y. Kim, K. Lee, G. T. Kim, G. S. Duesberg, T. Hallam, J. J. Boland, J. J. Wang, J. F. Donegan, J. C. Grunlan, G. Moriarty, A. Shmeliov, R. J. Nicholls, J. M. Perkins, E. M. Grieveson, K. Theuwissen, D. W. McComb, P. D. Nellist, and V. Nicolosi, Science **331**, 568 (2011).
[82] H. Steinberg, J. B. Laloe, V. Fatemi, J. S. Moodera, and P. Jarillo-Herrero, Phys. Rev. B **84**, 233101 (2011).
[83] M. Lang, L. He, F. Xiu, X. Yu, J. Tang, Y. Wang, X. Kou, W. Jiang, A. V. Fedorov, and K. L. Wang, ACS Nano **6**, 295 (2011).
[84] H. Cao, J. Tian, I. Miotkowski, T. Shen, J. Hu, S. Qiao, and Y. P. Chen, Phys. Rev. Lett. **108**, 216803 (2012).
[85] J. W. McIver, D. Hsieh, H. Steinberg, P. Jarillo Herrero, and N. Gedik, Nature Nano. **7**, 96 (2012).
[86] D. Kim, S. Cho, N. P. Butch, P. Syers, K. Kirshenbaum, S. Adam, J. Paglione, and M. S. Fuhrer, Nature Phys. **8**, 460 (2012).
[87] M. Veldhorst, M. Snelder, M. Hoek, T. Gang, V. K. Guduru, X. L. Wang, U. Zeitler, W. G. van der Wiel, A. A. Golubov, H. Hilgenkamp, and A. Brinkman, Nature Mater. **11**, 417 (2012).
[88] L. Fu and C. L. Kane, Phys. Rev. Lett. **100**, 096407 (2008).
[89] E. Majorana, Nuovo Cimento **5**, 171 (1937).
[90] F. Wilczek, Nature Phys. **5**, 614 (2009).
[91] J. Wang, C.-Z. Chang, H. Li, K. He, D. Zhang, M. Singh, X.-C. Ma, N. Samarth, M. Xie, Q.-K. Xue, and M. H. W. Chan, Phys. Rev. B **85**, 045415 (2012).
[92] J. R. Williams, A. J. Bestwick, P. Gallagher, S. S. Hong, Y. Cui, A. S. Bleich, J. G. Analytis, I. R. Fisher, and D. Goldhaber-Gordon, Phys. Rev. Lett. **109**, 056803 (2012).
[93] M. Veldhorst, C. G. Molenaar, X. L. Wang, H. Hilgenkamp, and A. Brinkman, Appl. Phys. Lett. **100**, 072602 (2012).
[94] D. Zhang, J. Wang, A. M. DaSilva, J. S. Lee, H. R. Gutierrez, M. H. W. Chan, J. Jain, and N. Samarth, Phys. Rev. B **84**, 165120 (2011).
[95] M. T. Deng, C. L. Yu, G. Y. Huang, M. Larsson, P. Caroff, and H. Q. Xu, arXiv:1204.4130v1 (2012).
[96] K. Nomura and N. Nagaosa, Phys. Rev. Lett. **106**, 166802 (2011).
[97] J. G. Checkelsky, J. Ye, Y. Onose, Y. Iwasa, and Y. Tokura, Nature Phys. **8**, 729 (2012).
[98] D. Kong, J. J. Cha, K. Lai, H. Peng, J. G. Analytis, S. Meister, Y. Chen, H.-J. Zhang, I. R. Fisher, Z.-X. Shen, and Y. Cui, ACS Nano **5**, 4698 (2011).

[99] M. Bianchi, R. C. Hatch, Z. Li, P. Hofmann, F. Song, J. Mi, B. B. Iversen, Z. M. Abd El-Fattah, P. Löptien, L. Zhou, A. A. Khajetoorians, J. Wiebe, R. Wiesendanger, and J. W. Wells, ACS Nano **6**, 7009 (2012).
[100] M. Bianchi, D. Guan, S. Bao, J. Mi, B. B. Iversen, P. D. C. King, and P. Hofmann, Nature Commun. **1**, 128 (2010).
[101] P. D. C. King, R. C. Hatch, M. Bianchi, R. Ovsyannikov, C. Lupulescu, G. Landolt, B. Slomski, J. H. Dil, D. Guan, J. L. Mi, E. D. L. Rienks, J. Fink, A. Lindblad, S. Svensson, S. Bao, G. Balakrishnan, B. B. Iversen, J. Osterwalder, W. Eberhardt, F. Baumberger, and P. Hofmann, Phys. Rev. Lett. **107**, 096802 (2011).
[102] M. Lang, L. He, F. Xiu, X. Yu, J. Tang, Y. Wang, X. Kou, W. Jiang, A. V. Fedorov, and K. L. Wang, ACS Nano **6**, 295 (2012).
[103] T. Gang, M. D. Yilmaz, D. Atac, S. K. Bose, E. Strambini, A. H. Velders, M. P. de Jong, J. Huskens, and W. G. van der Wiel, Nature Nano. **7**, 232 (2012).
[104] J. H. Bardarson, P. W. Brouwer, and J. E. Moore, Phys. Rev. Lett. **105**, 156803 (2010).
[105] K. J. Koski, J. J. Cha, B. W. Reed, C. D. Wessells, D. Kong, and Y. Cui, J. Am. Chem. Soc. **134**, 7584 (2012).
[106] K. J. Koski, C. D. Wessells, B. W. Reed, J. J. Cha, D. Kong, and Y. Cui, J. Am. Chem. Soc. **134**, 13773 (2012).
[107] H. D. Li, Z. Y. Wang, X. Kan, X. Guo, H. T. He, Z. Wang, J. N. Wang, T. L. Wong, N. Wang, and M. H. Xie, New J. Phys. **12**, 103038 (2010).
[108] A. Richardella, D. M. Zhang, J. S. Lee, A. Koser, D. W. Rench, A. L. Yeats, B. B. Buckley, D. D. Awschalom, and N. Samarth, Appl. Phys. Lett. **97**, 262104 (2010).
[109] S. A. Morin, A. Forticaux, M. J. Bierman, and S. Jin, Nano Lett. **11**, 4449 (2011).
[110] Y. Ran, Y. Zhang, and A. Vishwanath, Nature Phys. **5**, 298 (2009).
[111] K.-I. Imura, Y. Takane, and A. Tanaka, Phys. Rev. B **84**, 035443 (2011).
[112] O. A. Tretiakov, A. Abanov, and J. Sinova, Appl. Phys. Lett. **99**, 113110 (2011).